JOURNAL OF MOLECULAR SPECTROSCOPY 170, 82–93 (1995)

Infrared Emission Spectroscopy of BF and AlF

K.-Q. ZHANG, B. GUO, V. BRAUN, M. DULICK, AND P. F. BERNATH

Centre for Molecular Beams and Laser Chemistry, Department of Chemistry, University of Waterloo, Waterloo, Ontario, Canada N2L 3G1

The high-resolution infrared emission spectrum of boron monofluoride was recorded with a Fourier transform spectrometer. There are 359 transitions of ^{11}BF with $v = 1 \rightarrow 0$ to $v = 5 \rightarrow 4$, and 94 transitions of ^{10}BF with $v = 1 \rightarrow 0$ to $v = 3 \rightarrow 2$ assigned. Improved Dunham Y_{ij} coefficients for the ground $X\,^1\Sigma^+$ electronic state were determined from the infrared data combined with existing microwave data. The mass-reduced Dunham U_{ij} coefficients were also obtained along with Born–Oppenheimer breakdown constants. An effective Born–Oppenheimer potential was determined by fitting the available data to the eigenvalues of the radial Schrödinger equation containing a parameterized potential function. Finally, the relative transition dipole moments of the major isotopomer ^{11}BF were also measured. For AlF, our previous measurements were extended to higher v and J, in order to obtain improved Dunham coefficients and an improved internuclear potential.

I. INTRODUCTION

Since the BF spectrum was first observed by Dull (*1*) in 1935, BF has been subject to numerous spectroscopic studies. The electronic emission spectra of BF were recorded in many laboratories (*2–11*), but it was not until 1969 that Caton and Douglas (*9*) studied electronic absorption spectra of BF. In their report, Caton and Douglas gave an excellent overview of the electronic spectra. They not only clarified the assignments of the electronic states, but also they observed a series of Rydberg states approaching the ionization limit, which enabled them to determine the ionization potential (IP) very accurately. Their value of IP (11.115 ± 0.004 eV) agrees well with the values obtained from electron impact mass spectrometry (11.06 ± 0.10 eV) (*12*) and photoelectron spectroscopy (11.12 ± 0.01 eV) (*13*). Lovas and Johnson (*14*) recorded the first microwave spectrum of BF. They measured the $J = 1$–0 transitions of ^{11}BF and ^{10}BF and analyzed the hyperfine structure. They reported a dipole moment for $v = 0$ of 0.5 ± 0.2 D for BF. Recently, Cazzoli *et al.* (*15*) extended the frequency coverage of the microwave spectrum and obtained more transitions. Nakanaga *et al.* (*16*) measured 12 vibration–rotation transitions of the ^{11}BF fundamental band using a diode laser. The vibrational band strength of ^{11}BF was measured, and the value of $d\mu/dr$ was found to be 4.9 ± 0.8 D/Å (*31*).

Since BF is a member of the interesting isoelectronic group of molecules N_2, CO, and BF, several detailed theoretical calculations (*17–24*) of the properties of the ground and excited states have also been carried out. The spectroscopic constants are in good agreement with the experimental values, including the value for $d\mu/dr$. The value of the calculated dipole moment is about twice the experimental value, so it has been suggested that Lovas and Johnson underestimated μ_0 in their experiment.

In this study, we recorded and analyzed the vibration–rotation spectrum of the fundamental and several hot bands of ^{11}BF and ^{10}BF. During the course

0022-2852/95 $6.00

of our measurements, an improved spectrum of AlF was recorded as an impurity. We therefore take this opportunity to update the AlF constants and potential.

II. EXPERIMENTAL DETAILS

BF was generated inadvertently during our spectroscopic study of the CaF (*25*) free radical. A mixture of a trace amount of boron and 40 g of CaF_2 powder was contained in a carbon boat, which was placed in a reaction cell. The reaction cell consisted of a 1.2-m-long alumina (Al_2O_3) tube sealed with two KRS-5 windows at both ends. The alumina tube was further protected from the corrosive effects of the CaF_2 salt by a carbon liner tube. The central portion of the cell was situated inside a CM Rapid Temp furnace. The cell was first heated under vacuum up to 500°C, and was then pressurized with 5 Torr of argon to prevent condensation of vapor on the windows. When the cell temperature reached 1600°C, a strong emission of BF was detected.

The high-resolution spectrum of BF was recorded at a resolution of 0.01 cm^{-1} with a Bruker IFS 120 HR Fourier transform spectrometer at the University of Waterloo. A liquid-nitrogen-cooled HgCdTe detector, a KBr beamsplitter, and a KRS-5 entrance window were used. The lower limit of the spectral bandpass was set by the detector response at 850 cm^{-1}, while the upper limit was set by a red-pass optical filter with a cut-off wavenumber of 1670 cm^{-1}. The final spectrum of BF was a result of coadding 40 scans in about 40 min. A section of the spectrum is shown in Fig. 1. The AlF emission spectrum was obtained in a similar manner except that a Si:B photodetector was used.

III. RESULTS AND DISCUSSION

Since BF_3 was present in the cell when the spectrum was taken, part of the *R* branches of ^{11}BF and all of the *R* branches of ^{10}BF were buried in the absorption of the ν_3 band of BF_3.

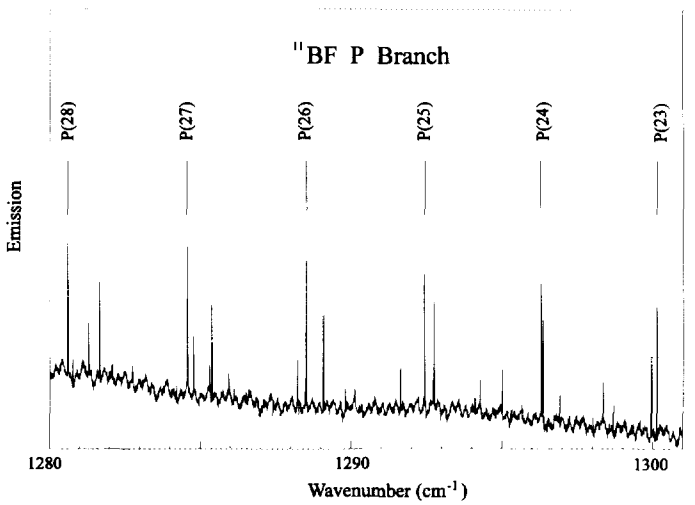

FIG. 1. Expanded view of the *P* branch of the BF $v = 1 \rightarrow 0$ band.

TABLE I

Observed Line Positions of ^{11}BF and ^{10}BF (in cm^{-1})

J'	J"	Observed	O-C[a]	SIG	J'	J"	Observed	O-C	SIG
^{11}BF									
				v = 1→0 band					
61	62	1127.1319	-01	02	60	61	1132.1236	04	02
59	60	1137.0882	81	05	58	59	1142.0243	-02	02
57	58	1146.9338	-04	02	56	57	1151.8171	06	05
55	56	1156.6714	04	02	54	55	1161.4972	-03	02
53	54	1166.2960	-01	02	52	53	1171.0662	-02	02
51	52	1175.8083	00	02	50	51	1180.5218	03	02
49	50	1185.2057	-01	02	48	49	1189.8618	05	05
47	48	1194.4876	01	02	46	47	1199.0844	02	02
45	46	1203.6515	00	02	44	45	1208.1892	02	02
43	44	1212.6967	01	02	42	43	1217.1738	-02	02
40	41	1226.0380	-00	02	39	40	1230.4239	-01	02
38	39	1234.7794	00	02	37	38	1239.1038	01	02
36	37	1243.3965	-01	02	35	36	1247.6584	-00	02
34	35	1251.8885	-00	02	33	34	1256.0868	-01	02
32	33	1260.2534	-00	02	31	32	1264.3878	-00	02
30	31	1268.4898	-01	02	29	30	1272.5598	01	02
28	29	1276.5967	-00	02	27	28	1280.6011	01	02
26	27	1284.5721	-01	02	25	26	1288.5101	-01	02
24	25	1292.4151	-00	02	23	24	1296.2865	01	02
22	23	1300.1238	-01	02	21	22	1303.9275	-01	02
20	21	1307.6972	-01	02	19	20	1311.4326	-01	02
18	19	1315.1336	-00	02	17	18	1318.8002	00	02
16	17	1322.4317	-02	02	15	16	1326.0286	-00	02
14	15	1329.5903	-00	02	13	14	1333.1171	03	02
12	13	1336.6078	00	02	11	12	1340.0632	01	02
10	11	1343.4829	03	02	9	10	1346.8658	-03	08
8	9	1350.2129	-07	08	7	8	1353.5244	-03	08
6	7	1356.7993	-00	08	5	6	1360.0381	07	08
4	5	1363.2379	-06	08	3	4	1366.4025	-02	08
2	3	1369.5289	-08	08	1	2	1372.6214	21	08
1	0	1381.6645	20	08	2	1	1384.6041	30	30
3	2	1387.5009	-05	08	4	3	1390.3637	02	08
5	4	1393.1875	06	08	6	5	1395.9718	01	08
7	6	1398.7173	-02	08	8	7	1401.4250	06	08
9	8	1404.0926	05	08	10	9	1406.7201	-02	08
12	11	1411.8595	14	08	13	12	1414.3672	00	08
14	13	1416.8358	-04	08	16	15	1421.6545	07	08
18	17	1426.3052	-38	30	19	18	1428.5772	18	30
23	22	1437.2276	-14	08	28	27	1447.1073	03	08
				v = 2→1 band					
59	60	1116.6685	48	30	58	59	1121.5448	-14	03
57	58	1126.3999	-19	30	56	57	1131.2303	00	02
55	56	1136.0317	04	03	54	55	1140.8057	09	08
53	54	1145.5503	-02	02	52	53	1150.2686	02	02
51	52	1154.9566	-14	08	50	51	1159.6189	-06	03
49	50	1164.2525	00	02	48	49	1168.8571	04	03
47	48	1173.4316	-03	02	46	47	1177.9776	-06	04
45	46	1182.4952	-01	02	44	45	1186.9828	-01	02
43	44	1191.4411	01	02	42	43	1195.8695	03	02
41	42	1200.2671	-02	02	40	41	1204.6367	13	08

a) observed minus calculated values in units of 10^{-4} cm^{-1}.

The rotational lines were measured using the computer program PC-DECOMP developed by J. W. Brault. The line positions were determined by fitting the measured line profiles to Voigt lineshape functions. The pure rotational lines of HF which were present in the spectra as an impurity were used to calibrate the BF and AlF spectra (*32*). The error in the calibrated line positions is estimated to be 0.0002 cm^{-1} for ^{11}BF and 0.0005 cm^{-1} for ^{10}BF and AlF. Five bands of ^{11}BF from $v = 1 \rightarrow 0$ to $v = 5 \rightarrow 4$ are analyzed, while three bands of ^{10}BF from $v = 1 \rightarrow 0$ to $v = 3 \rightarrow 2$ are studied. The line positions are given in Table I.

TABLE I—*Continued*

J'	J"	Observed	O-C	SIG	J'	J"	Observed	O-C	SIG
39	40	1208.9730	-00	02	38	39	1213.2801	-01	02
37	38	1217.5567	01	02	36	37	1221.8022	01	02
35	36	1226.0166	01	02	34	35	1230.1998	02	02
33	34	1234.3510	-02	02	32	33	1238.4716	03	02
31	32	1242.5599	03	02	30	31	1246.6156	-01	02
29	30	1250.6400	02	02	28	29	1254.6315	00	02
27	28	1258.5903	-02	02	26	27	1262.5169	-01	02
25	26	1266.4105	-01	02	24	25	1270.2711	00	02
23	24	1274.0983	00	02	22	23	1277.8917	-02	02
21	22	1281.6522	00	02	20	21	1285.3787	01	02
19	20	1289.0709	-00	02	18	19	1292.7295	02	02
17	18	1296.3531	-01	02	16	17	1299.9426	-00	02
15	16	1303.4974	-01	02	14	15	1307.0177	02	02
13	14	1310.5026	01	02	12	13	1313.9524	01	02
11	12	1317.3657	-09	08	10	11	1320.7456	00	02
9	10	1324.0887	00	02	8	9	1327.3961	01	02
7	8	1330.6672	00	02	6	7	1333.9020	-01	02
5	6	1337.1005	-02	02	4	5	1340.2621	-06	03
3	4	1343.3869	-11	08	1	0	1358.4609	36	30
3	2	1364.2217	-00	02	4	3	1367.0473	03	02
6	5	1372.5836	12	08	7	6	1375.2911	-11	08
8	7	1377.9629	-03	03	9	8	1380.5956	02	02
10	9	1383.1897	13	08	11	10	1385.7421	00	02
12	11	1388.2560	-04	03	13	12	1390.7315	04	02
14	13	1393.1666	06	03	15	14	1395.5604	-05	02
16	15	1397.9168	10	08	17	16	1400.2301	-02	02
18	17	1402.5042	-02	02	19	18	1404.7379	-01	02
20	19	1406.9300	-07	03	21	20	1409.0829	02	02
22	21	1411.1927	-07	03	23	22	1413.2627	-02	02
25	24	1417.2775	-01	02	27	26	1421.1253	00	02
28	27	1422.9870	08	03					
				v = 3-2 band					
55	56	1115.7269	21	08	54	55	1120.4446	-03	03
53	54	1125.1369	-06	08	52	53	1129.8037	10	05
51	52	1134.4394	-05	03	50	51	1139.0503	10	05
49	50	1143.6302	-01	02	48	49	1148.1834	03	02
47	48	1152.7072	-00	02	46	47	1157.2045	18	30
45	46	1161.6686	-04	02	44	45	1166.1061	-03	02
43	44	1170.5148	03	02	42	43	1174.8931	01	02
41	42	1179.2420	01	02	40	41	1183.5608	00	02
39	40	1187.8497	-00	02	38	39	1192.1075	-08	03
37	38	1196.3368	02	02	36	37	1200.5344	02	02
35	36	1204.7009	-00	02	34	35	1208.8372	04	02
33	34	1212.9409	-06	03	32	33	1217.0145	-02	02
31	32	1221.0564	-01	02	30	31	1225.0669	02	02
29	30	1229.0447	-01	02	28	29	1232.9907	-02	02
27	28	1236.9048	-00	02	26	27	1240.7865	02	02
25	26	1244.6352	01	02	24	25	1248.4508	-02	02
23	24	1252.2341	-00	02	22	23	1255.9842	02	02
21	22	1259.7004	-02	02	20	21	1263.3834	-02	02
19	20	1267.0332	01	02	18	19	1270.6484	-00	02
17	18	1274.2300	00	02	16	17	1277.7772	00	02
15	16	1281.2905	03	02	14	15	1284.7684	00	02

A. Dunham Model

We determined ^{11}BF and ^{10}BF Dunham Y_{ij} coefficients from the observed line positions from a linear least-squares fit. Microwave measurements of the ^{11}BF and ^{10}BF pure rotational transitions, with hyperfine structure corrected by Cazzoli *et al.* (*15*), were also added as input to the linear fit. The Dunham coefficients for both isotopomers are listed in Table II, while the mass-reduced Dunham U_{ij} coefficients are listed in Table III. In Table III, under the column heading "unconstrained," the U_{ij} coefficients were obtained from a combined fit of isotopomer data to the expression

$$E(v, J) = \sum_{i,j} \mu^{-(i/2+j)} U_{ij} \left(1 + \frac{m_e}{M_A}\Delta_{ij}^A + \frac{m_e}{M_B}\Delta_{ij}^B\right)\left(v + \frac{1}{2}\right)^i [J(J+1)]^j, \quad (1)$$

TABLE I—*Continued*

J'	J"	Observed	O-C	SIG	J'	J"	Observed	O-C	SIG
13	14	1288.2120	01	02	12	13	1291.6206	-00	02
11	12	1294.9937	-04	02	10	11	1298.3328	03	02
9	10	1301.6348	-04	02	8	9	1304.9021	-03	02
7	8	1308.1334	-06	03	6	7	1311.3282	-12	08
5	6	1314.4884	-04	02	4	5	1317.6104	-14	08
3	4	1320.6980	-04	03	2	3	1323.7488	03	02
0	1	1329.7397	20	08	1	0	1335.5790	06	03
3	2	1341.2694	04	02	4	3	1344.0611	34	30
7	6	1352.1952	02	02	8	7	1354.8296	-10	08
9	8	1357.4263	-13	08	10	9	1359.9891	32	30
11	10	1362.5050	00	02	12	11	1364.9857	06	03
13	12	1367.4260	02	02	14	13	1369.8294	25	30
15	14	1372.1884	00	02	16	15	1374.5097	-03	02
17	16	1376.7921	03	02	18	17	1379.0326	-06	03
19	18	1381.2345	-00	02	20	19	1383.3949	-04	02
21	20	1385.5145	-08	05	22	21	1387.5949	01	02
23	22	1389.6333	01	02	24	23	1391.6323	18	30
25	24	1393.5864	00	02	26	25	1395.4990	-19	30
27	26	1397.3730	-08	08	29	28	1400.9954	09	05
30	29	1402.7438	21	30	31	30	1404.4479	12	05
34	33	1409.3086	17	08	36	35	1412.3334	04	10
				v = 4-3 band					
50	51	1118.8200	-07	08	49	50	1123.3496	05	08
48	49	1127.8473	-19	10	47	48	1132.3251	36	30
46	47	1136.7668	15	08	45	46	1141.1806	01	02
44	45	1145.5665	-03	03	43	44	1149.9251	06	03
42	43	1154.2523	-05	04	41	42	1158.5524	05	03
40	41	1162.8207	-07	03	39	40	1167.0608	-03	02
38	39	1171.2717	07	03	37	38	1175.4501	-06	03
36	37	1179.5995	-08	05	35	36	1183.7193	00	02
34	35	1187.8073	-02	02	33	34	1191.8655	04	02
32	33	1195.8919	03	02	31	32	1199.8858	-09	05
30	31	1203.8510	04	02	29	30	1207.7833	05	03
28	29	1211.6834	02	02	26	27	1219.3880	-00	02
25	26	1223.1922	02	02	24	25	1226.9628	-07	03
23	24	1230.7019	-03	02	22	23	1234.4077	-06	02
21	22	1238.0800	-11	04	20	21	1241.7209	00	02
19	20	1245.3278	06	03	18	19	1248.8990	-09	05
17	18	1252.4393	04	02	16	17	1255.9436	-03	02
15	16	1259.4141	-06	03	14	15	1262.8520	04	02
13	14	1266.2543	06	03	12	13	1269.6212	-00	02
11	12	1272.9537	-02	02	10	11	1276.2520	01	02
9	10	1279.5145	00	02	8	9	1282.7424	06	03
7	8	1285.9343	07	03	6	7	1289.0894	-02	02
4	5	1295.2945	01	02	3	4	1298.3463	39	30
2	1	1315.8559	-56	30	3	2	1318.6514	-02	02
4	3	1321.4056	14	08	5	4	1324.1167	-22	30
6	5	1326.7939	-19	30	7	6	1329.4343	-04	02
8	7	1332.0355	00	02	9	8	1334.5996	18	30
10	9	1337.1221	05	03	11	10	1339.6066	00	02
12	11	1342.0528	-00	02	13	12	1344.4591	-08	03
14	13	1346.8285	05	03	15	14	1349.1569	03	02
17	16	1353.6961	11	08	18	17	1355.9036	-08	03

where m_e is the electron mass, M_A and M_B are masses for atoms A and B, and the Δ_{ij}'s are Born–Oppenheimer breakdown constants. Since only one naturally occurring isotope of fluorine exists, all isotopic information on Born–Oppenheimer breakdown is confined to the boron atom. Therefore, only Δ_{ij}'s for the boron atom were determined from the least-squares fit of the data. Finally, the set of U_{ij}'s under the column heading "constrained" in Table III were obtained from a fit where the U_{ij}'s for $j \leq 1$ were treated as independent parameters, while all remaining U_{ij}'s were fixed to values determined from the constraint relations implicit in the Dunham model (*29*). The reduced χ^2 of the "unconstrained" and "constrained" fits are 0.9727 and 0.9667, respectively. We believe that the constrained fit is more meaningful since it uses fewer

TABLE I—*Continued*

J'	J"	Observed	O-C	SIG	J'	J"	Observed	O-C	SIG
19	18	1358.0738	-02	02	21	20	1362.2922	-01	02
22	21	1364.3406	-02	02	23	22	1366.3495	07	03
24	23	1368.3139	-18	30	25	24	1370.2419	00	02
26	25	1372.1278	09	05	27	26	1373.9714	08	03
28	27	1375.7716	-12	05	31	30	1380.9300	06	03
32	31	1382.5643	-00	02	33	32	1384.1575	03	03
34	33	1385.7070	-05	02	35	34	1387.2131	-23	10
36	35	1388.6796	-10	05					
				v = 5-4 band					
44	45	1125.3707	-10	10	42	43	1133.9564	-00	02
40	41	1142.4262	10	05	39	40	1146.6174	17	10
38	39	1150.7797	32	20	34	35	1167.1199	-02	02
32	33	1175.1087	-09	08	31	32	1179.0580	-01	02
28	29	1190.7149	-11	08	27	28	1194.5383	-06	05
25	26	1202.0895	03	02	24	25	1205.8160	-00	02
23	24	1209.5069	-36	20	22	23	1213.1718	-06	05
21	22	1216.8016	00	02	20	21	1220.3980	00	02
19	20	1223.9621	09	05	18	19	1227.4907	-02	02
17	18	1230.9874	00	02	16	17	1234.4526	24	10
15	16	1237.8777	-15	08	14	15	1241.2741	-01	02
13	14	1244.6352	00	02	12	13	1247.9596	-20	08
11	12	1251.2549	11	10	10	11	1254.5122	11	10
9	10	1257.7346	09	10	7	8	1264.0744	09	10
6	7	1267.1929	24	30	3	4	1276.3210	-63	30
4	3	1299.0780	-60	60	6	5	1304.4171	19	30
8	7	1309.5860	06	10	9	8	1312.1119	-15	08
10	9	1314.6055	22	30	11	10	1317.0555	07	10
12	11	1319.4685	09	10	13	12	1321.8442	23	30
14	13	1324.1824	53	30	15	14	1326.4695	-37	30
16	15	1328.7329	25	30	17	16	1330.9452	-27	30
26	25	1349.1068	-18	30	27	26	1350.9257	18	10
30	29	1356.1223	02	02					
^{10}BF									
				v = 1-0 band					
52	53	1198.6323	02	03	50	51	1208.7774	03	03
49	50	1213.8035	08	05	48	49	1218.7951	-17	08
47	48	1223.7589	-05	02	46	47	1228.6883	-18	08
45	46	1233.5891	04	05	44	45	1238.4555	05	05
43	44	1243.2887	-00	02	42	43	1248.0898	00	02
41	42	1252.8574	-04	03	40	41	1257.5939	10	05
39	40	1262.2938	-07	05	38	39	1266.9630	02	05
37	38	1271.5983	12	05	36	37	1276.1981	05	05
35	36	1280.7636	-02	05	34	35	1285.2957	-01	05
33	34	1289.7932	00	05	32	33	1294.2554	-04	05
31	32	1298.6837	01	02	30	31	1303.0765	04	03
29	30	1307.4331	-00	02	28	29	1311.7551	03	02
27	28	1316.0408	01	02	26	27	1320.2898	-06	03
25	26	1324.5038	-03	03	24	25	1328.6815	00	05
23	24	1332.8218	-03	03	22	23	1336.9257	-03	03
21	22	1340.9941	10	08	20	21	1345.0233	04	05

parameters. Indeed the Δ_{ij}^{B} parameters for the constrained fit have much more reasonable values.

B. Parameterized Potential Model

In order to estimate information on the high-lying rovibrational levels of the ground state, a reliable internuclear potential energy function is required. Such a potential function can be determined from a least-squares fit (*29*) of the combined ^{11}BF and ^{10}BF data to the eigenvalues of the radial Schrödinger equation

$$\left(\frac{\hbar^2}{2\mu}\nabla^2 - U^{\text{eff}}(R) + E(v, J) - \frac{\hbar^2}{2\mu}[1 + q(R)]\frac{J(J+1)}{R^2}\right)\psi(R, v, J) = 0, \quad (2)$$

TABLE I—*Continued*

J'	J"	Observed	O-C	SIG	J'	J"	Observed	O-C	SIG
19	20	1349.0137	-15	08	18	19	1352.9702	00	05
17	18	1356.8858	-14	08	16	17	1360.7682	18	20
15	16	1364.6074	00	05	14	15	1368.4104	03	08
13	14	1372.1727	-12	30	11	12	1379.5902	45	20
10	11	1383.2330	01	30					
				v = 2-1 band					
43	44	1220.7806	-11	08	41	42	1230.2428	02	02
40	41	1234.9239	-00	02	39	40	1239.5761	39	30
38	39	1244.1872	-01	02	37	38	1248.7684	-05	05
36	37	1253.3172	01	02	35	36	1257.8305	-06	05
34	35	1262.3110	-02	05	33	34	1266.7574	03	02
32	33	1271.1693	07	05	31	32	1275.5451	-01	05
30	31	1279.8863	-08	05	29	30	1284.1934	-05	05
28	29	1288.4655	-00	02	27	28	1292.7011	-05	05
26	27	1296.9021	00	02	25	26	1301.0662	-04	02
24	25	1305.1959	08	05	23	24	1309.2864	-08	05
22	23	1313.3433	03	02	21	22	1317.3657	36	30
20	21	1321.3444	02	05	19	20	1325.2901	08	05
18	19	1329.1974	02	05	17	18	1333.0678	04	05
16	17	1336.8978	-22	30	15	16	1340.6937	-11	05
14	15	1344.4591	75	50	13	14	1348.1706	05	08
12	13	1351.8513	12	10	11	12	1355.4917	02	10
10	11	1359.0936	-02	10	9	10	1362.6569	-03	10
7	8	1369.6651	-11	08					
				v = 3-2 band					
37	38	1226.2873	-02	50	35	36	1235.2548	00	10
34	35	1239.6855	25	20	33	34	1244.0784	13	20
31	32	1252.7639	10	10	30	31	1257.0541	01	05
29	30	1261.3097	-06	05	28	29	1265.5325	07	05
27	28	1269.7182	01	02	26	27	1273.8683	-06	03
24	25	1282.0623	-15	08	23	24	1286.1059	-15	08
22	23	1290.1149	00	02	21	22	1294.0868	08	08
20	21	1298.0203	-00	02	19	20	1301.9172	-08	08
18	19	1305.7790	02	02	17	18	1309.6038	14	08
16	17	1313.3902	15	08	15	16	1317.1370	-02	05
14	15	1320.8494	12	08	13	14	1324.5205	-05	08
10	11	1335.3099	-03	02	8	9	1342.3097	01	02

where the effective internuclear potential for vibrational motion is given by

$$U^{\text{eff}}(R) = U^{\text{BO}}(R) + \frac{U_A(R)}{M_A} + \frac{U_B(R)}{M_B}, \tag{3}$$

TABLE II

Dunham Y_{ij} Coefficients for ^{10}BF and ^{11}BF (in cm^{-1})

Coefficient	^{10}BF	^{11}BF
Y_{10}	1445.6660(10)	1402.15865(26)
Y_{20}	-12.57365(61)	-11.82106(15)
Y_{30}	0.059565(97)	0.051595(35)
10^3Y_{40}	-	3.464(29)
Y_{01}	1.61228632(86)	1.51674399(21)
Y_{11}	-0.0208783(16)	-0.01904848(22)
10^4Y_{21}	6.736(92)	5.8464(76)
10^6Y_{31}	1.38(13)	1.2899(73)
10^6Y_{02}	-8.0208(59)	-7.09528(35)
10^6Y_{12}	1.191(48)	0.9605(52)
10^6Y_{22}	0.74(16)	1.05(14)

TABLE III

Mass-Reduced Dunham Coefficients and Born–Oppenheimer Breakdown Constants for the Boron Atom (in cm^{-1})

Constant	Unconstrained	Constrained
U_{10}	3701.6995(32)	3701.6938(21)
U_{01}	-82.3937(10)	-82.39384(97)
U_{20}	0.94859(64)	0.94852(63)
U_{11}	0.01702(14)	0.01707(14)
U_{02}	10.572952(33)	10.572893(22)
U_{21}	-0.350748(61)	-0.350606(13)
$10^{1}U_{12}$	2.8422(37)	2.8540(25)
$10^{1}U_{03}$	1.6520(94)	1.6134(88)
$10^{1}U_{30}$	-3.4673(73)	-3.45017003
$10^{2}U_{31}$	1.2359(68)	1.30362995
$10^{2}U_{22}$	3.518(47)	3.04905340
$10^{2}U_{13}$		1.39465056
$10^{2}U_{04}$		7.31811680
$10^{3}U_{41}$		2.86741980
$10^{3}U_{32}$		4.31289760
$10^{3}U_{23}$		-1.44942336
$10^{3}U_{14}$		1.97762269
$10^{3}U_{05}$		1.95249239
$10^{4}U_{50}$		-2.29286491
$10^{4}U_{41}$		2.54097932
$10^{4}U_{32}$		1.06645896
$10^{4}U_{23}$		1.40418786
$10^{4}U_{14}$		2.04263339
$10^{4}U_{05}$		1.99636817
Δ^{B}_{10}	0.832(17)	0.865(10)
Δ^{B}_{01}	-1.838(61)	-1.718(40)
Δ^{B}_{11}	-12.3(34)	-3.38(65)
Δ^{B}_{02}	-116.(42)	-7.62(83)

and the form of the Born–Oppenheimer potential is chosen to be

$$U^{\mathrm{BO}}(R) = D_e\left[\frac{1 - e^{-\beta(R)}}{1 - e^{-\beta(\infty)}}\right]^2, \tag{4}$$

where

$$\beta(R) = z \sum_{i=0} \beta_i z^i \tag{5}$$

$$\beta(\infty) = \sum_{i=0} \beta_i \tag{6}$$

and

$$z = \frac{R - R_e}{R + R_e}. \tag{7}$$

The remaining terms in Eq. (3) are corrections for atomic nuclei A and B which take into Born–Oppenheimer breakdown and homogeneous nonadiabatic mixing from distant Σ electronic states and are represented by the power series expansions

$$U_A(R) = \sum_{i=1} u_i^A (R - R_e)^i \tag{8}$$

and

$$U_B(R) = \sum_{i=1} u_i^B (R - R_e)^i. \tag{9}$$

TABLE IV

Internuclear Potential Energy Parameters for BF

Parameter	Value	Uncertainity
$D_e/10^4$ cm^{-1}	6.36	
R_e/Å	1.262711672	4.23×10^{-7}
β_0	4.51429026	2.30×10^{-6}
β_1	1.4509287	5.42×10^{-7}
β_2	0.098562	8.13×10^{-4}
β_3	3.8626	1.48×10^{-2}
β_4	26.402	1.42×10^{-1}
β_5	69.05	1.74
u^B_1/cm^{-1}Å^{-1}	-208.93	1.93
u^B_2/cm^{-1}Å^{-2}	790.04	5.41
u^B_3/cm^{-1}Å^{-3}	-310.16	4.27
M_A(^{19}F)/amu	18.99840322	
M_B(^{11}B)/amu	11.0093054	
M_B(^{10}B)/amu	10.0129369	

Similarly, effects from rotational motion, namely, J-dependent Born–Oppenheimer breakdown and heterogeneous nonadiabatic mixing from distant II electronic states, are accounted for by the $q(R)$ term in Eq. (2) where

$$q(R) = \frac{1}{M_A}\sum_{i=1} q_i^A (R - R_e)^i + \frac{1}{M_B}\sum_{i=1} q_i^B (R - R_e)^i. \tag{10}$$

Our fitting procedure is similar to the method reported by Coxon and Hajigeorgiou (*27, 28*) and is described in greater detail elsewhere (*29, 30*). None of the q parameters could be determined using our data set. Results of the potential fit are given in Table IV. The potential energy curve of BF is shown in Fig. 2. Potential parameters that were statistically determined are listed along with their uncertainties quoted to one standard deviation. The value of D_e was fixed to that given in Huber and Herzberg (*34*). The standard deviation of the fit is 1.5864.

The analysis of AlF spectrum was similar to that of BF. Hot bands of AlF up to $v = 9 \rightarrow 8$ were measured. The updated Dunham coefficients for AlF are listed in Table

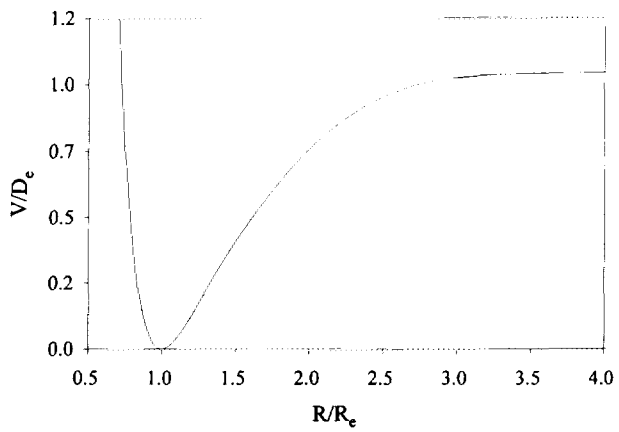

FIG. 2. The Born–Oppenheimer potential energy for BF (ground state).

TABLE V

Dunham Y_{ij} Coefficients for AlF (in cm^{-1})

Coefficient	This Work	Ref. (33)
Y_{10}	802.32447(11)	802.32385(15)
Y_{20}	-4.849915(44)	-4.849536(98)
Y_{30}	0.0195738(68)	0.019497(24)
$10^3 Y_{40}$	3.407(35)	2.95(20)
Y_{01}	0.552480208(65)	0.552480296(49)
$10^3 Y_{11}$	-4.984261(44)	-4.984214(60)
$10^5 Y_{21}$	1.7215(95)	1.7153(22)
$10^8 Y_{31}$	4.022(57)	5.03(24)
$10^9 Y_{02}$	-1.047999(51)	-1.048280(68)
$10^9 Y_{12}$	1.7814(93)	1.8548(80)
$10^{11} Y_{22}$	6.578(75)	3.01(19)
$10^{13} Y_{03}$	-3.674(49)	-3.050(93)
$10^{13} Y_{13}$	9.55(74)	-

V together with those reported in Ref. (*33*). Although the highest vibrational energy level accessed is $v = 5$ in the previous work (*33*) while transitions involving up to $v = 9$ were measured in this study, the changes in the Dunham coefficients are very small. This indicates that the Dunham model is adequate for a moderately heavy molecule such as AlF. A parameterized potential was also determined, and the potential energy parameters for AlF are given in Table VI. The value of D_e was also fixed to that given in Huber and Herzberg (*34*).

C. *Relative Transition Dipole Moment*

The experimental intensity parameters are very important in the evaluation of abundances and temperatures of gaseous species by spectroscopic means. Measuring line intensities is also important for the understanding of the variation of the molecular dipole moment with respect to normal coordinates, i.e., the dipole moment function (*35*). However, rovibrational line intensities of free radicals are difficult to measure because of the small and uncertain column densities.

In our spectroscopic study of BF, we obtained a relatively high signal-to-noise spectrum (Fig. 1), thus enabling us to investigate the line intensities of BF. Since there was no means of obtaining the concentration of BF available in our laboratory, only the relative intensities of the ^{11}BF rotational lines were measured. Due to the fact that

TABLE VI

Internuclear Potential Energy Parameters for AlF

Parameter	Value	Uncertainity
$D_e/10^4$ cm^{-1}	5.60	
R_e/Å	1.6543689056	6.95×10^{-9}
β_0	4.561386175	4.87×10^{-9}
β_1	0.4435571	2.62×10^{-7}
β_2	0.805792	1.88×10^{-4}
β_3	8.12058	7.96×10^{-3}
β_4	11.0386	5.02×10^{-2}
$M_A(^{19}F)$/amu	18.99840322	
$M_B(^{27}Al)$/amu	26.9815386	

TABLE VII

Relative Transition Dipole Moments of ^{11}BF

Band	Relative Transition Dipole Moment		
	This Work	Ref.(24)	Ref.(22)
1→0	1	1	1
2→1	1.42	1.44	1.44
3→2	1.71	1.78	1.79
4→3	2.13	-	2.10

the transmission of the optics, the efficiency of the beamsplitter, and the response of the detector vary with frequency, a narrow wavenumber range was chosen. The choice of wavenumber range was somewhat arbitrary, but we chose it in such a way that there were intense lines within the range, and the line intensities could be measured readily; i.e., there were no blended lines and the continuum level could be determined to a high degree of accuracy. Consequently, the range between 1280 and 1300 cm^{-1} was selected. Since the $v = 5 \rightarrow 4$ band is weak, only four bands from $v = 1 \rightarrow 0$ to $v = 4 \rightarrow 3$ were compared. Equation (3) in Ref. (*26*) was applied to convert rotational line intensities to transition dipole moments. The measured average transition dipole moments were normalized to that of $v = 1 \rightarrow 0$ band; their values are listed in Table VII together with the *ab initio* predictions obtained from Refs. (*24, 22*). There is a good agreement between our experimental values and the *ab initio* results. The *ab initio* calculations of the dipole moment function are clearly of high quality.

IV. CONCLUSION

Fourier transform infrared emission spectroscopy is a very useful technique for recording high resolution vibration–rotation spectra of high temperature molecules. Our infrared data on ^{11}BF and ^{10}BF, together with existing microwave data, were converted to spectroscopic constants in two ways. The first approach utilized the traditional Dunham model extended to include data from different isotopomers. It is evident that imposing constraints on the Dunham coefficients improves consistency among the parameters. The second approach employed a parameterized potential model which uses a direct comparison between the experimental data and the solution to the Schrödinger equation. The second model can predict higher-lying rotation–vibration energy levels of the electronic ground state that are at least qualitatively correct. The traditional Dunham model is inadequate when extrapolating far beyond the range of experimental measurements. Finally, the relative transition moments were also measured, and the values agree with the *ab initio* calculation satisfactorily. Provided that spectra with good signal-to-noise ratios are available, the relative transition dipole moments of other transient molecules can be determined, and possibly also the dipole moment functions.

ACKNOWLEDGMENTS

This work was supported by the Natural Sciences and Engineering Council of Canada (NSERC). KQZ thanks NSERC for a scholarship.

RECEIVED: August 29, 1994

REFERENCES

1. R. B. DULL, *Phys. Rev.* **47,** 458–465 (1935).
2. M. CHRETIEN AND E. MIESCHER, *Nature* **163,** 996–997 (1949).
3. M. CHRETIEN, *Helv. Phys. Acta* **23,** 259–286 (1950).
4. R. ONAKA, *J. Chem. Phys.* **27,** 374–377 (1957).
5. R. F. BARROW, D. PREMASWARUP, J. WINTERNITZ, AND P. B. ZEEMAN, *Proc. Phys. Soc. London A* **71,** 61–63 (1958).
6. D. W. ROBINSON, *J. Mol. Spectrosc.* **11,** 275–300 (1963).
7. S. L. N. G. KRISHNAMACHARI AND M. SINGH, *Current Sci. (India)* **34,** 655–660 (1965).
8. J. CZARNY AND P. FELENBOK, *Chem. Phys. Lett.* **2,** 533–535 (1968).
9. R. B. CATON AND A. E. DOUGLAS, *Can. J. Phys.* **48,** 432–452 (1970).
10. A. C. LE FLOCH, J. LEBRETON, F. LAUNAY, J. FERRAN, AND J. ROSTAS, *J. Phys. B* **13,** 3989–3992 (1980).
11. H. BREDOHL, I. DUBOIS, F. MÉLEN, AND M. VERVLOET, *J. Mol. Spectrosc.* **129,** 145–150 (1988).
12. D. L. HILDENBRAND, *Int. J. Mass Spectrom. Ion Phys.* **7,** 255–260 (1971).
13. J. M. DYKE, C. KIRBY, AND A. MORRIS, *J. Chem. Soc. Faraday Trans. 2* **79,** 483–490 (1983).
14. F. J. LOVAS AND D. R. JOHNSON, *J. Chem. Phys.* **55,** 41–44 (1971).
15. G. CAZZOLI, L. CLUDI, C. D. ESPOSTI, AND L. DORE, *J. Mol. Spectrosc.* **134,** 159–167 (1989).
16. T. NAKANAGA, H. TAKEO, S. KONDO, AND C. MATSUMURA, *Chem. Phys. Lett.* **114,** 88–91 (1985).
17. R. K. NESBET, *J. Chem. Phys.* **40,** 3619–3633 (1964).
18. R. K. NESBET, *J. Chem. Phys.* **43,** 4403–4409 (1965).
19. W. M. HUO, *J. Chem. Phys.* **43,** 624–647 (1965).
20. H. LEFEBVRE-BRION AND C. M. MOSER, *J. Mol. Spectrosc.* **15,** 211–219 (1965).
21. H. A. KURTZ AND K. D. JORDON, *Chem. Phys. Lett.* **81,** 104–109 (1981).
22. P. ROSMUS, H.-J. WERNER, AND M. GRIMM, *Chem. Phys. Lett.* **92,** 250–256 (1982).
23. P. BOTSCHWINA, *J. Mol. Spectrosc.* **118,** 76–87 (1986).
24. M. HONIGMANN, G. HIRSCH, AND R. J. BUENKER, *Chem. Phys.* **172,** 59–71 (1993).
25. F. CHARRON, B. GUO, K.-Q. ZHANG, Z. MORBI, AND P. F. BERNATH, *J. Mol. Spectrosc.* (submitted for publication).
26. E. E. WHITING, A. SCHADEE, J. B. TATUM, J. T. HOUGEN, AND R. W. NICHOLLS, *J. Mol. Spectrosc.* **80,** 249–256 (1980).
27. J. A. COXON AND P. G. HAJIGEORGIOU, *Can. J. Phys.* **70,** 40–54 (1992).
28. J. A. COXON AND P. G. HAJIGEORGIOU, *Chem. Phys.* **167,** 327–340 (1992).
29. H. G. HEDDERICH, M. DULICK, AND P. F. BERNATH, *J. Chem. Phys.* **99,** 8363–8370 (1993).
30. M. DULICK AND P. F. BERNATH, in preparation.
31. M. S. ZAHNISER AND M. E. GERSH, *J. Chem. Phys.* **75,** 52–58 (1981).
32. R. B. LEBLANC, J. B. WHITE, AND P. F. BERNATH, *J. Mol. Spectrosc.* **164,** 574–579 (1994).
33. H. R. HEDDERICH AND P. F. BERNATH, *J. Mol. Spectrosc.* **153,** 73–80 (1992).
34. K. P. HUBER AND G. HERZBERG, "Constants of Diatomic Molecules," Van Nostrand-Reinhold, New York, 1979.
35. M. A. H. SMITH, C. P. RINSLAND, B. FRIDOVICH, AND K. NARAHARI RAO, *in* "Molecular Spectroscopy: Modern Research" (K. Narahari Rao, Ed.), Vol. III, pp. 111–248, Academic Press, New York, 1985.